Quantitative Analysis Method forBacterial Cells in SEM Image using Deep Learning

Anonymous ECCV submission

Paper ID 12

Abstract. In this paper we propose a method to segment, classify and quantitatively analyze bacteria from a given Scanning Electron Microscope (SEM) image of the bacterial sample. Thousands of bacteria lives in the human gut and recent studies have shown that the quantitative features of the microbiome, such as co-existence ratio of different bacteria, can be indicative of the health condition in humans. Therefore, to realize a system to quantitatively analyze the gut bacteria of humans, we propose a method to segment, classify and calculate the ratio of the bacteria contents for a few well-known bacteria types. Our method achieves more than 90% recall for all of original three datasets. Additionally, we also introduce a novel image processing based touching object separation algorithm which is applied within the framework of our system. Subsequently, we show the comparison results between another state-of-the-art segmentation method and the introduced algorithm and we empirically report that our new algorithm has a better performance.

Keywords: bacteria, SEM, segmentation, classification, neural network

1 Introduction

In the recent years there's mounting evidence [5, 6, 12] that thousands of different types of bacteria inhabiting all of us, known collectively along with their genetic material as the microbiome, is crucial to our survival, influencing every aspect of health from our daily mood to body weight. Therefore, it is utmost necessary that these bacteria which reside inside the human gut be analyzed for further investigation. However, there are hardly any effective techniques that comes to one's mind for this purpose. The current techniques of counting cells include naked eye inspection, use of automatic colony counters, viable growth counting methods or the measurement of the microbial mass.

Therefore, in this research, we propose to identify bacterium by morphological features in high resolution image taken by Scanning Electron Microscope (SEM). By this method, we expect that we can analyze bacteria in greater detail than conventional analysis method.

In the current general observation of bacteria, optical microscope is used. Also, in the conventional image processing method for counting bacteria, the target is colony of cultured single type of bacteria. The conventional method will analyze the size or number of colony, not bacteria type [2]. However, our

target domain is SEM image which has more high resolution, it include visual feature of membrane or inside of bacteria. Therefore, we propose a method to classify and quantitatively analyze bacteria from a given SEM image.

In this research, we verified the usefulness of our method using three original datasets which consisted 6 bio-cultured bacteria types. The results of this study suggest that our method may be applied to all human microbiota studies, mainly gut, skin, etc. in the future.

1.1 Related Works

In the field of computer vision, semantic segmentation is the field of research where the end goal is to classify each pixel in a given image to its respective object class. Semantic segmentation is a high-level task that paves the way towards complete scene understanding. The importance of scene understanding as a core computer vision problem is highlighted by the fact that an increasing number of applications nourish from inferring knowledge from imagery.

The most popular way of doing semantic segmentation, using CNN, approach has been through the fully convolutional approach where instead of a linear combination learning layer at the end, which predicts the class of each pixel at a time, we use a convolutional layer at the end which performs a 1×1 convolution to predict the pixel label at once. Since [9], the SegNet [1] has been a popular architecture to use the deconvolutional method for up sampling the high-level features into a class wise map.

In cellular image segmentation, especially the ones that are taken by an electron microscope has always been a challenging problem because of several reasons such as irregular shape of cells, tightly pack colonies, shape and textural similarities between different type of bacterium, etc. In addition, the dataset sizes in the biomedical domain has always remained an issue. To address some of the issues mentioned above, the ISBI EM segmentation challenge [8] was launched which resulted in some developments in the EM media segmentation. Namely, a system by Ciresan et al. [3] which took the sliding-window approach won the 2012 competition. However, there were some problems with the system like huge computational cost, etc. However, the one system that won the 2015 competition and addressed the maximum number of problems was the U-Net [10]. U-Net is very versatile because it follows the Fully Convolutional concept making it robust to input sizes, hardware constraints, and high computationally efficient compared with sliding-window approach. Another noticeable property of the U-Net is skip connections. Skip connection helps to identify with more high accuracy using high-level feature which has information from large area and low-level feature which has specific local information.

1.2 Existing Bottleneck

Although deep learning based segmentation systems perform very well in identifying the class of an object, they suffer from reconstructing the correct border

in case the cells are too close or actually having some overlap. This problem is shown with the help of a representative Fig. 1.

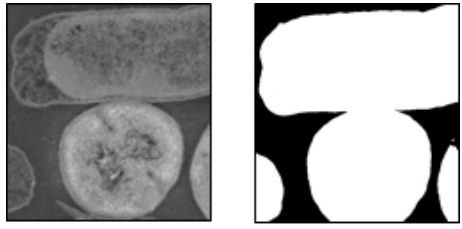

Fig. 1. (a) An Example Image of bacteria cells from Bacteria Set 3 where the cells are actually touching each other. (b) An example of binary segmentation result.

To tackle this problem, the conventional U-Net uses a pixel-wise loss weight map during the model optimization process to magnify the penalty for higher loss in pixels situated in the border of the cells. This method requires many situations of touching cells to learn a considerable distribution accurately. However, number of bacteria images are limited, and it is difficult to control location of bacterium in the SEM images. However, in the real-world deployment, such an assumption might be fatal. Also, in case of our dataset, which already have very few samples to start with, in addition, there are not enough cases of samples with touching cells that a good distribution can be learned from. However, the problem of touching cells still exists in our case (Fig. 1) and can greatly hamper the classification and counting process. In particular, in some of the cases, the cells were actually touching each other without any background pixels in between. In those cases, the model fails to separate the cells completely. However, we want to separate bacteria region to calculate quantitative information of bacteria (for example, the number or ratio of each type of bacteria). So, we propose a post processing method to separate touching object in binary images.

Therefore, the contributions of this paper are the following:

- A framework to segment, classify and quantitatively analyze the gut bacteria from SEM images
- An image-processing based touching object separation algorithm from binary mask images.

2 Methodology

To realize our overall target of counting and calculating the ratio in the given bacterial image sample, we have broken down the process into four distinct modules – (1) Segmentation module, (2) Separation module, (3) Classification module, (4) Counting module as shown in Fig. 2.

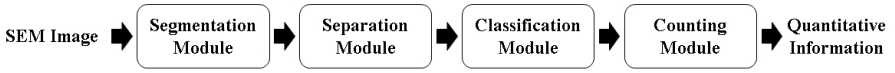

Fig. 2. The modules in the proposed method.

2.1 Segmentation Module

The segmentation module categorizes the image region into foreground and background region.

Table 1. List of hyperparameter settings used in our model

Hyper Parameter	Value
Base Learning rate	0.0001
Learning Policy	RMSProp [7]
Decay	0.99
CNN Kernel Size	3×3
MAX Pool Kernel Size	2×2
Deconvolution Kernel Size	2×2

The main purpose of the segmentation module is to create regions of interest in the sample image where the bacterial cells are located. In the segmentation process, this is done by categorizing the bacterial sample image region into background region and the foreground region. The segmentation process helps the classifier to have higher confidence of classification accuracy by providing the prior knowledge of the classification area. The segmentation is done using a fully convolutional approach using U-Net [10] which performs a pixel-wise binary segmentation of the bacterial sample image. The U-Net is trained using the image-label pair. Where the label is a map containing the correct area of foreground and background region. We used the original U-Net architecture from the original paper. The hyperparameters used in our model are listed in Table 1.

2.2 Separation Module

The separation unit on the other hand is responsible for separating the touching cells so that the cells can be represented individually for quantitative analysis. Though our model can often separate the closely situated cells that have an actual border between them, it still fails to separate the cells that are touching (Fig. 1).

Also, the problem of touching cells poses a great amount of threat to our research objective. Therefore, we wanted to address this problem in a coherent and a redundant manner which makes the separation as accurate as possible. Therefore, we developed a method for efficient separation of the touching cells.

Our separation method spans in two parts. The first part is localized watershed transform method, The second part is shape-wise separation method. Details will be described later, the localized watershed transform is effective

when the object is circular and two bacteria are touch with a small area (Fig. 3(a)). On the other hand, since the shape-wise separation focuses only on the shape features around the touching area, it is possible to separate without depending on the overall shape and touching area size (Fig. 3(b)). However, since the shape-wise separation is difficult to separate the touching cells on the border (Fig. 3(c)) because this method needs to shape information both sides of the touching area. the localized watershed method is more robust to separate bacteria on the border. So we adopted both method. Green arrows are expected separation point.

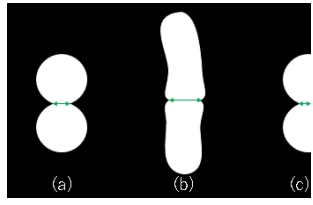

Fig. 3. Examples of touching bacteria. (a) is case of circular bacteria touch with a small area (both separate methods will separate well.) (b) is case of non-circular bacteria touch with large area (shape-wise separation is more effective.) (c) is case of touching bacteria are on border (localized watershed is more effective.)

Therefore, the process of our separation algorithm in the current scenario works in the following steps:

1. Receive an inference map from the model and perform localized watershed transform on the foreground region which touched image border.
2. On the output map from step 1, perform the shape-wise separation algorithm for the foreground region which does not touch the image border.

The Localized Watershed Transform

Watershed algorithm [4] is well known as one of the popular segmentation method for binary image. It separate touching region by spreading region from core regions using distance map which is calculated by distance transformation[11]. In normal watershed algorithm, core regions are extracted by thresholding using distance map and fixed thresholding value. But in our target, it is difficult to decide the fixed thresholding value because the size of bacteria varies.

So, we normalize distance map by dividing by maximum distance of each connected region. After that, we extract core regions by thresholding with fixed value (form 0.0 to 1.0). We call this method as the localized watershed transform.

The localized watershed transformation technique is applied to the regions shown in regions Fig. 4(a). In this part we first isolate each region separately and then we perform the localized distance transform of that region. After that, we perform thresholding to retain the seed area (Fig. 4(b)) in that region. After that we expand the seed regions until they meet each other. The meeting point is considered to be the border between them (Fig. 4(c)). This step is especially

useful in the case of peripheral cells which does not have a symmetry in the touching regions.

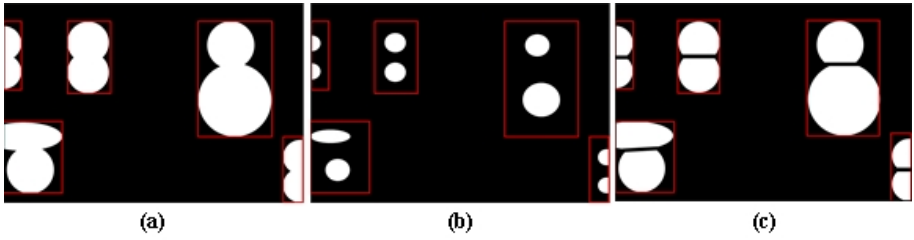

Fig. 4. A set of representation diagrams showing the local watershed transform method (a) The region to be separated (b) The seed regions are generated through distance transform and thresholding (c) The cells are separated using watershed transform of the seeds.

The Shape-Wise Separation Touching Cells

The shape-wise separation model is the original algorithms developed in this research. First, we begin with the distance transform of the entire inference map and get the distance map (not localized.) At this point, the relative brightness level of all foreground pixels represents the distance to the nearest background pixel as shown in Fig. 5(b). Our aim is to search for pixels that are situated at the bridge regions as indicated with p in Fig. 5.

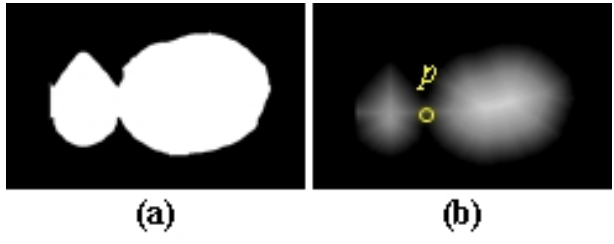

Fig. 5. The image of (a) an inference map of an image and (b) the distance map of every foreground pixel. The distance to the background is denoted by the brightness of the pixel. Point p is bridge region.

For each foreground pixel, we perform the Algorithm 1 to find the pixels at the touching regions (known as the bridge pixels). Where p is target pixel of this task, axis A is axis rotated by θ from horizontal axis, axis B is axis rotated by 90 degree from axis A, b_r and b_l is nearest background pixel from pixel p with direction of positive and negative side in axis B, $f_r b_r$ and $f_l b_r$ is nearest foreground pixel of b_r with direction of positive and negative side in axis A, $f_r b_l$ and $f_l b_l$ is nearest foreground pixel of b_l with direction of negative and positive side in axis A and α is threshold value for distance of nearest foreground pixel of b . Sometimes, we simply denote b to represent b_r or b_l. In same sense, $f_r b$ represents $f_r b_l$ or $f_r b_r$, and $f_l b$ represents $f_l b_r$ or $f_l b_r$ also.

Algorithm 1 Shape-Wise Separation

Require: Segmentation result and Distance map
Ensure: Segmentation result which separated touching cells
  Input Segmentation result copy to O
  for each pixel p **do**
    for each rotation θ **do**
      if pixel p satisfy following conditions:
      - Brightness along the axis A of the location p is consistent
      - Brightness along the axis B of the location p is consistent and lower than pixel p **then**
        if b_r and b_l satisfy following conditions:
        - Nearest foreground pixel of b: $f_r b$ within the α
        - Nearest foreground pixel of b: $f_l b$ within the α
        - The pixel along axis B of b is a background pixel with in the α **then**
          join b_r and b_l with a black line in O
        end if
      end if
    end for
  end for
  Output O

2.3 The Classification Module

Once the touching regions have been successfully separated using the elaborate separation mechanism described above, we use a class wise classifier on the final foreground region to classify them to their respective bacteria classes. This classifier is a traditional patch wise classifier. The optimal patch size that was choses in of size 200×200 pixels. Classifier is based on VGG-16.

This network basically takes an image and based on the foreground identified by segmentation module and separation module, spatially slides the model in a sliding window fashion to classify each patch in the image. The network finally outputs the probabilities of the class according to the patches. After that, we adopt majority class in each bacteria region identified by segmentation and separation module as final classification result.

2.4 Cell Counting

After classifying the bacteria into their respective classes, the counting was conducted which is essential to the end goal of this research and also required for ratio calculation. The count was done by selecting each foreground region and by examining the color code of that region as shown in Fig. 6. We count each isolated foreground region as one bacteria region.

3 Experimental Result

3.1 Dataset Preparation

We have developed following three bacteria datasets. Each No. indicate a kind of bacteria.

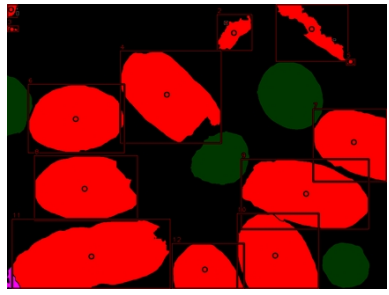

Fig. 6. A representation diagram showing the detection for counting of cells belonging to the class corresponding to red color.

- **Bacteria Set 1**: Consists of two kinds of Bacteria – No.1 and No.2. These bacteria are distinguishable comparatively in our bacteria datasets.
- **Bacteria Set 2**: Consists of another two kinds of Bacteria – No.4 and No.7. No.4 and No.7 are similar and more difficult to distinguish than Bacteria Set 1
- **Bacteria Set 3**: Consists of six kinds of Bacteria (Set1, Set2 along with two new kinds) – No.1, No.2, No.4, No.5, No.7 and No.8. This variant of our dataset is the most challenging one because it has a larger number of bacteria types, and among them, many of the bacteria types share similar visual features like shape, texture, etc.

These datasets have been specifically prepared through bio-culture of the bacteria found in the human gut. Each dataset had around 100 SEM images with resolution of 960×1280 pixels and gray scale. We had made pixel wise annotation data manually. For training of U-Net, we have generated patches of the images of size 400×400 pixels. For training of classifier, we also used some basic data augmentation techniques such as rotation and flipping. The classification was performed on the foreground region of the data with a sliding window approach of patch size 200×200 pixels where the ground truth label of the center pixel was used as the training label for the patch. Table 2 shows number of bacteria which are included each dataset and mean size of each bacteria type in training data. However, note that the mean size of bacteria is smaller than the actual bacteria size because bacteria on the image boundary are also included in the mean size calculation.

3.2 Evaluation Criteria

We adopt as final evaluation criteria, pixel accuracy for segmentation result. The detailed formula for the pixel accuracy for class c is given in equation 1. For overall evaluation, we use mean pixel accuracy and total pixel accuracy as well. These are given in equation 2 and 3. In the pixel accuracy for evaluation of segmentation, TP stands for true foreground, TN stands for true background, FP stands for false foreground and FN stands for false background. Suffix c indicates class index and C indicates number of classes.

Table 2. Number and Size of cells

	Number of Bacteria			Mean Size of
	Bacteria Set1	Bacteria Set2	Bacteria Set3	Bacteria [pixel]
No1	236	-	286	49971
No2	290	-	542	29874
No4	-	46	52	42926
No5	-	-	201	45054
No7	-	292	123	45439
No8	-	-	208	48118
Total	526	338	1412	(ave)43563

$$Pixel\ Accuracy(c) = \frac{(TP_c + TN_c)}{(TP_c + TN_c + FP_c + FN_c)} \tag{1}$$

$$Mean\ Pixel\ Accuracy = \sum_c (PixelAccuracy(c))/C \tag{2}$$

$$Total\ Pixel\ Accuracy = \frac{\sum_c (TP_c + TN_c)}{\sum_c (TP_c + TN_c + FP_c + FN_c)} \tag{3}$$

For classification evaluation, we adopt recall and average Absolute Difference of bacteria Ratio (ADR). Recall is given in equation 4. In the recall, TP stands for true positive, FP stands for false positive and FN stands for false negative for each class. The false positive in this case was calculated based on the distance of the center of the prediction and the ground truth. We first compute the prediction of the central region of every cell and compare it with foreground label of the ground truth. If there is no specific type of bacteria situated in the prediction in 100-pixel radius from the center pixel as the ground truth label, we consider it as false negative (FN). Likewise, if there is a specific type of bacteria in the prediction and the same does not appear within 100-pixels center radius in the ground truth label, we consider it as false positive (FP).

$$Recall(c) = \frac{TP_c}{(TP_c + FN_c)} \tag{4}$$

ADR is calculated from bacteria ratio of ground truth and detection result. Bacteria ratio of ground truth is calculated by equation 5 and bacteria ratio of detection result is calculated by equation 6. Where TP_c, FN_c and FP_c indicate TP, FN and FP of class C. TP, FN and FP are same as case of recall explained above.

$$Bacteria\ Ratio\ of\ Ground\ Truth = \frac{(TP_c + FN_c)}{\sum(TP_c + FN_c)} \tag{5}$$

$$Bacteria\ Ratio\ of\ Detection\ Result = \frac{(TP_c + FP_c)}{\sum(TP_c + FP_c)} \tag{6}$$

3.3 Experiments

To test our methods and hypotheses, we conducted experiments extensively on the different datasets described in Section 3.1. Fig. 7 shows an example that input and each output of module in our proposed method. In Fig. 7(c), each detected bacteria region colored according to classified result. As you can see, our method can detect each bacteria region separately, and has classified each bacteria region into it respective classes encoded in different colors.

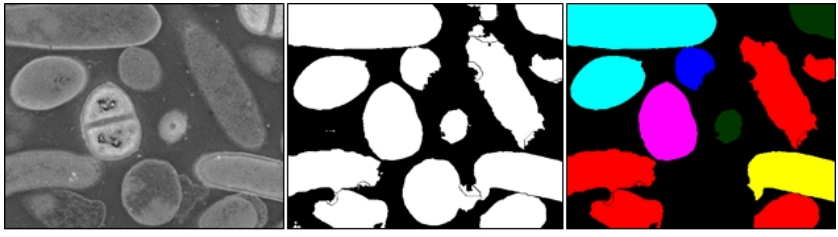

Fig. 7. The overall processing pipeline starting with (a) The input image (b) the foreground-background segmented and separated region (c) The final output from the classifier which has successfully classified each foreground region into its respective classes encoded in different colors.

Table 3 shows that pixel accuracy for Bacteria Set 1, 2 and 3 respectively. In Table 3, 1st and 2nd column indicate pixel accuracy for background and bacteria region, 3rd column indicate mean pixel accuracy of background and bacteria region, and 4th column indicate pixel accuracy for all pixels in the evaluation image. We have achieved more than 90% pixel accuracy and mean accuracy.

Table 3. The evaluation result of segmentation

Bacteria Set	Pixel Accuracy of Background region [%]	Pixel Accuracy of Bacteria region [%]	Mean Accuracy [%]	Pixel Accuracy [%]
1	96.16	96.41	96.29	96.23
2	89.54	97.29	93.42	92.52
3	88.84	98.40	93.62	91.91

Table 4, 5 and 6 show that confusion matrix and recall of each dataset. And table 7, 8 and 9 show that ADR of each dataset. Recall and ADR are already introduced in Section 3.2.

4 Considerations

4.1 Comparison with the Conventional Method

Let us now consider the comparison of our results with result of conventional U-Net method using Bacteria Set 3. In Section 1.2 we have talked about the

Table 4. Confusion Matrix of the Bacteria Set 1

		Detected				Recall[%]
		No1	No2	missing	total	
Label	No1	64		1	65	98.5
	No2		56		56	100
	Total	64	56	1	121	99.2

Table 5. Confusion Matrix of the Bacteria Set 2

		Detected				Recall[%]
		No4	No7	missing	total	
Label	No4	14	1	2	17	82.4
	No7		146	4	150	97.3
	Total	14	147	6	167	95.8

Table 6. Confusion Matrix of the Bacteria Set 3

		Detected								Recall[%]
		No1	No2	No4	No5	No7	No8	missing	total	
Label	No1	51		4					55	92.7
	No2	1	58		1		4		64	92.2
	No4	1		1					2	50.0
	No5				9				9	100
	No7				1	11		1	13	84.6
	No8		2		1		23	2	28	82.1
	Total	53	60	5	12	11	27	3	171	90.1

conventional U-Net model which use weight map for learning the border regions. In this section we perform experiments to show how the conventional U-Net compare with our proposed method. Table 10 and Table 11 shows the result of pixel accuracy and recall of conventional U-Net on the Bacteria Set 3. By comparison of Table 3 and Table 10, you can see that both of pixel accuracy and mean accuracy of proposed method are higher than conventional method. Table 11 clearly show accuracy of the proposed method is higher than accuracy of the conventional U-Net. We also found that in the conventional U-Net model, there were more than usual holes (Fig. 8(a) (b)) being generated in the foreground region which may be due to the fact that many border areas which has higher penalties due to the weight map share similar features with a lot of foreground region as well. Also, we found that there were cases where in spite of weight map, the touching cells could not be separated (Fig. 8(c) (d)).

4.2 Evaluation of Separation Module

We evaluate effect of both of separation method: localized watershed transform and shape-wise separation method. Table 12 shows the relationship between the presence or absence of each method and the recall. In Table 12, localize watershed transform is denoted as WS and shape-wise separation denoted as SW-sep. The both of separation method improved total recall by 20% or more compared to the case without them.

Table 7. The result of detection and ratio on the Bacteria Set 1

	Bacteria Ratio[%]		
	Ground Truth	Detected	ADR
No1	53.7	85.2	4.5
No2	46.3	41.8	4.5
Total	100	100	(ave)4.5

Table 8. The result of detection and ratio on the Bacteria Set 2

	Bacteria Ratio[%]		
	Ground Truth	Detected	ADR
No4	10.2	9.7	0.5
No7	89.8	90.3	0.5
Total	100	100	(ave)0.5

Table 9. The result of detection and ratio on the Bacteria Set 3

	Bacteria Ratio[%]		
	Ground Truth	Detected	ADR
No1	32.2	41.9	9.7
No2	37.4	27.5	9.9
No4	1.2	2.3	1.2
No5	5.3	7.0	1.7
No7	7.6	7.0	0.6
No8	16.4	14.3	2.0
Total	100	100	(ave)4.2

5 Conclusion

We have proposed a technique for efficiently identifying and counting and calculating the ratio of gut bacteria from a given SEM image. In this context, we have considered a state-of-the-art method known as the U-Net for object segmentation in a given SEM image. We have outlined the problems of the conventional U-Net model.

We have conducted experiments with three datasets – Bacteria Set 1, Bacteria Set 2 and Bacteria Set 3 and we have achieved total recall accuracy of 99.2%, 95.8% and 90.1% on the given datasets respectively. We have also achieved absolute difference of ratio between ground truth and detection result less than 5% for all datasets we prepared.

In this research, we used the kinds of bacteria sample that was bio-cultured in the lab. However, our goal of this research is applying to bacterial sample from the human gut in the future. We would like to address the challenge of miss-classification and miss-separation in our method to increase the precision as well. We will improve our method to apply to all human microbiota, mainly gut, skin, etc.

Table 10. The evaluation result of segmentation by conventional U-Net

Bacteria Set	Pixel Accuracy of Background region [%]	Pixel Accuracy of Bacteria region [%]	Mean Accuracy [%]	Pixel Accuracy [%]
3	95.46	72.84	84.15	88.19

Table 11. The result of detection and ratio by the conventional U-Net on the Bacteria Set 3

	Recall[%]	Bacteria Ratio[%]		
		Ground Truth	Detected	ADR
No1	83.6(46/55)	32.2	47.6	15.5
No2	87.5(56/64)	37.4	23.4	14.0
No4	50.0(1/2)	1.2	2.6	1.4
No5	100(9/9)	5.3	5.9	0.6
No7	84.6(11/13)	7.6	7.3	0.3
No8	57.1(16/28)	16.4	13.2	3.2
Total	90.1(154/171)	100	100	(ave)5.8

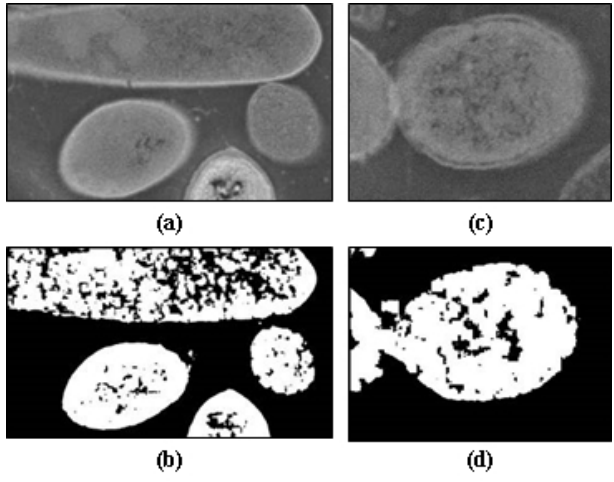

Fig. 8. (a) and (b) is a case which have a lot of holes generated in the foreground region. (c) and (d) is a case which include non-separation of touching cells in spite of using weight map. (a) and (c) The input image and (b) and (d) The generated inference map of the image by the conventional U-Net model.

Table 12. The evaluation result of Watershed and Shape-wise separation

	w/o WS and SW-sep[%]	SW-sep	WS	WS and SW-sep
No1	63.6(35/55)	87.3(48/55)	92.7(51/55)	96.4(53/55)
No2	81.3(52/64)	87.5(56/64)	90.6(58/64)	90.6(58/64)
No4	50(1/2)	50(1/2)	50(1/2)	50(1/2)
No5	88.9(8/9)	100(9/9)	100(9/9)	100(9/9)
No7	69.2(9/13)	76.9(10/13)	84.6(11/13)	84.6(11/13)
No8	53.6(15/28)	78.6(22/28)	78.6(22/28)	82.1(23/28)
Total	70.2(120/171)	85.4(146/171)	88.9(152/171)	90.6(155/171)

References

1. Badrinarayanan, V., Kendall, A., Cipoll, R.: Segnet: A deep convolutional encoder-decoder architecture for image segmentation (2017)
2. Brugger, S.D., Baumberger, C., Jost, M., Jenni, W., Brugger, U., Muhlemann, K.: Automated counting of bacterial colony forming units on agar plates (2012)
3. Ciresan, D.C., Giusti, A., Gambardella, L.M., Schmidhuber, J.: Deep neural networks segment neuronal membranes in electron microscopy images (2012)
4. Couprie, M., Bertrand, G.: Topological gray-scale watershed transformation (1997)
5. Gill, S.R., Pop, M., Deboy, R.T., Eckburg, P.B., Turnbaugh, P.J., Samuel, B.S., Gordon, J.I., Relman, D.A., Fraser-Liggett, C.M., Nelson, K.E.: Metagenomic analysis of the human distal gut microbiome (2006)
6. of Health, N.I.: Nih launches human microbiome project (2007), https://www.genome.gov/26524200/2007-release-nih-launches-human-microbiome-project
7. Hinton, G., Srivastava, N., Swersky, K.: Neural networks for machine learning, http://www.cs.toronto.edu/ tijmen/csc321/slides/lecture_slides_lec6.pdf
8. IEEE: Isbi challenge: Segmentation of neuronal structures in em (2012), http://brainiac2.mit.edu/isbi_challenge/home
9. Long, J., Shelhamer, E., Darrell, T.: Fully convolutional networks for semantic segmentation (2015)
10. Ronneberger, O., Fischer, P., Brox, T.: U-net: Convolutional networks for biomedical image segmentation (2015), arXiv preprint arXiv:1505.04597
11. Rosenfeld, A., Pfaltz, J.L.: Sequential operations in digital picture processing (1966)
12. Turnbaugh, P.J., Hamady, M., Yatsunenko, T., Cantarel, B.L., Duncan, A., Ley, R.E., Sogin, M.L., Jones, W.J., Roe, B.A., Affourtit, J.P., Egholm, M., Henrissat, B., Heath, A.C., Knight, R., Gordon, J.I.: A core gut microbiome in obese and lean twins (2008)